Ferromagnetic Resonance in Nickel Ferrite as a Function of Temperature*

D. W. HEALY, JR.†
Cruft Laboratory, Harvard University, Cambridge, Massachusetts
(Received January 16, 1952)

Ferromagnetic resonance in $NiOFe_2O_3$ has been studied over a temperature range of −195°C to 588°C. From this study the variation in line width with temperature, g value, and magnetic anisotropy constants K_1 and K_2 have been determined. Results show that the line width decreases with increasing temperature, the g value remains essentially constant, and the two anisotropy constants show different sign behavior over the temperature range.

I. INTRODUCTION

THE phenomenon of ferromagnetic resonance originally observed by Griffiths[1] has since received extensive study both theoretically[2,3] and experimentally.[4–7] In particular, Yager *et al.*[8] have studied the resonance phenomenon in single crystals of $NiOFe_2O_3$ at room temperature.

This paper discusses the experimental results of a study made on $NiOFe_2O_3$ over a temperature range of −195°C to 588°C. The Curie temperature of $NiOFe_2O_3$ is approximately 600°C. The investigation was carried out at a frequency of about 9000 Mc/sec on small spherical samples. These spheres were about 0.019 inch in diameter, and hence, were small enough so that the rf electromagnetic field could be considered uniform throughout their volume. In addition, their small size relative to the exciting wavelength insured the avoidance of dimensional resonance effects.

A study has been made of the line width of the resonance curve, the variation of the spectroscopic splitting factor, g, and the magnetic anisotropy constants, K_1 and K_2, as a function of temperature.

II. EXPERIMENTAL

The experimental technique of measurement was similar to that used by Bloembergen[7] in studying the resonance phenomenon in nickel and Supermalloy. A block diagram of the measuring equipment is shown in Fig. 1. A sample was placed in a rectangular microwave cavity excited by a fixed frequency rf field, and the power absorbed by the sample then was measured as a function of the magnitude of a constant magnetic field H_0. This field was so oriented that its lines of flux were perpendicular to those of the rf field.

In order to measure the power absorbed in the sample, the unloaded Q, Q_μ, of the cavity and the coupling Q, Q_e, were determined by conventional techniques. Q_μ at zero value of H_0 was measured both with the sample in the cavity and also without a sample. The two Q_μ's were nearly identical; therefore, the sample did not materially contribute to loss either of a dielectric or eddy current nature in the cavity. Since nickel ferrite has a high resistivity[9] and since the sample was located at a region of rf magnetic field maximum (electric field minimum), it is expected that such losses would be small.

Once Q_μ for the cavity and sample had been determined at zero H_0, the technique was to measure the power reflected from the cavity as a function of H_0. Since the power incident on the cavity was held constant, the variation in power absorbed in the sample could be found in terms of the power reflected from the cavity. The power absorbed in the cavity in turn could be expressed in terms of a change of the Q_μ of the cavity.

The imaginary component, μ'', of the permeability of the ferrite sample can be evaluated from a knowledge of the change in Q of the cavity by using a perturbation technique such as described by Bethe and Schwinger.[10] In order to employ this technique we must know the field configuration in the cavity and we must assume that the distortion of these fields produced by the

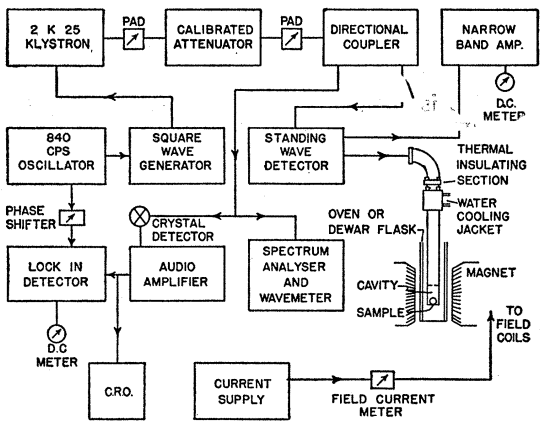

FIG. 1. Block diagram of measuring equipment.

* This work was supported by the ONR.
† Now at College of Applied Science, Syracuse University, Syracuse, New York.

[1] J. H. E. Griffiths, Nature **158**, 670 (1946).
[2] C. Kittel, Phys. Rev. **73**, 155 (1948).
[3] J. H. Van Vleck, Phys. Rev. **78**, 266 (1950).
[4] H. G. Beljers, Physica **14**, 629 (1949).
[5] A. F. Kip and R. D. Arnold, Phys. Rev. **75**, 1556 (1949).
[6] L. R. Bickford, Tech. Rept. XXIII Lab. Insulation Research MIT (October 1949).
[7] N. Bloembergen, Phys. Rev. **78**, 572 (1950).
[8] Yager, Galt, Merritt, and Wood, Phys. Rev. **80**, 744 (1950).
[9] J. L. Snoek, *New Developments in Magnetic Materials* (Elsevier Publishing Company, Houston, Texas, 1946).
[10] H. A. Bethe and J. Schwinger, Natl. Defense Research Committee Report D1-117, March 1943.

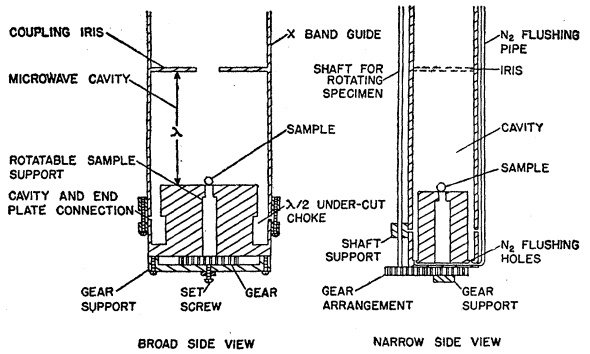

FIG. 2. Detail of microwave cavity.

introduction of the sample into the cavity is negligibly small. For this case we have

$$(\delta f/f)+j\delta(1/2Q_\mu)=\delta W/W, \tag{1}$$

where f is the resonant frequency of the cavity, δf the change in the resonant frequency produced by the introduction of the sample, Q_μ the unloaded Q of the cavity, δW the change in stored energy in the cavity produced by the introduction of the sample, and W is the total stored energy of the cavity. If we know the field configuration, we can compute W and also δW in terms of $\mu=\mu'+j\mu''$. In computing W and δW we take advantage of the fact that the sample was placed in a region of the cavity where the electric rf field is negligibly small.

By this means μ'' can be calculated from the relationship

$$\mu''=\frac{\Delta Q_\mu}{2Q_\mu^2}\frac{V}{\Delta V}\frac{\lambda_g^2}{2\lambda_1^2}, \tag{2}$$

where ΔQ is the change in the value of Q_μ measured as a function of the constant magnetic field, V is the volume of the cavity, ΔV the volume of the sample, λ_g is the resonant wavelength in the cavity, and λ_1 the free space wavelength corresponding to λ_g.

Figure 2 is a drawing showing the test cavity and sample. The sample was mounted so that it could be rotated about a [110] axis in the same fashion employed by Yager *et al.*[8] With this method of mounting the magnetic field H_0, which is perpendicular to the axis of rotation, will remain in a (110) plane of the crystal as the sample is rotated but will successively pass through the three principal crystallographic axes, the [100], [110], and [111] directions. The method of crystal alignment and mounting also was similar to that used by Yager *et al.* except that here the sample had to be held in place by a material that would withstand a large temperature variation. Insalute cement was used for this purpose.

Since the cavity was to be used over a wide temperature range it was necessary to prevent oxidation of the copper cavity walls at the high temperature and also prohibit the condensation of water vapor and oxygen at the low temperatures. For this purpose a slight positive pressure of dry nitrogen was maintained in the cavity at all times.

The spherical samples were prepared by a technique similar to that described by Bond.[11]

The steady magnetic field was measured in terms of the current through the field coils. The calibration of the magnetic field in terms of the field current was made by means of a proton resonance device of the type reported by Pound and Knight.[12]

III. THEORETICAL

Kittel has shown that the general resonance condition is

$$\omega=\gamma H_{\text{eff}}, \tag{3}$$

where γ is the gyromagnetic ratio, $g(e/2mc)$, and g is the spectroscopic splitting factor.[13] H_{eff}, the effective value of the constant magnetic field, is given by

$$H_{\text{eff}}=\{[H_0+(N_y+N_y^{a1}+N_y^{a2}-N_z)M_z] \times[H_0+(N_x+N_x^{a1}+N_x^{a2}-N_z)M_z]\}^{\frac{1}{2}}. \tag{4}$$

H_0 is the externally applied field, assumed here to be in the z direction, N_x, N_y, and N_z are the shape dependent demagnetizing factors, and N_x^{a1}, N_y^{a1} and N_x^{a2}, N_y^{a2} are effective demagnetizing factors introduced to account for the presence of magnetic anisotropy energy. Kittel[2] and Bickford[6] have shown that, when H_0 is in a (110) plane and is strong enough to saturate the sample magnetically, these effective demagnetizing factors are given by

$$\left.\begin{aligned} N_x^{a1}&=(1-\sin^2\theta-3\sin^2 2\theta)(K_1/M_z^2),\\ N_y^{a1}&=2(1-2\sin^2\theta-\tfrac{3}{8}\sin^2 2\theta)(K_1/M_z^2),\\ N_x^{a2}&=\tfrac{1}{2}\sin^2\theta(6\cos^4\theta-11\sin^2\theta\cos^2\theta \\ &\qquad +\sin^4\theta)(K_2/M_z^2),\\ N_y^{a2}&=-\tfrac{1}{2}\sin^2\theta\cos^2\theta(3\sin^2\theta+2)(K_2/M_z^2). \end{aligned}\right\} \tag{5}$$

Here θ measures the angle between H_0 and a [100] axis of the crystal, and K_1 and K_2 are the first and second order anisotropy constants, respectively. From

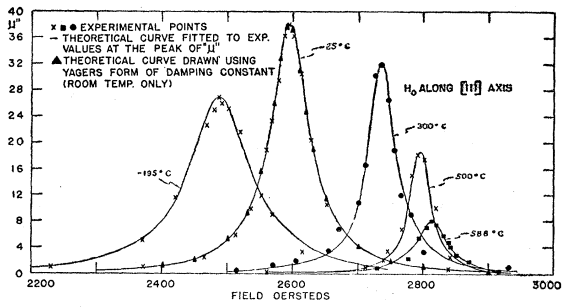

FIG. 3. μ'' *vs* H_0 for $NiOFe_2O_3$ single crystal sphere.

[11] W. L. Bond, Rev. Sci. Instr. **5**, 344 (1951).
[12] R. V. Pound and W. D. Knight, Rev. Sci. Instr. **21**, 219 (1950).
[13] C. Kittel, Phys. Rev. **76**, 743 (1949).

these expressions, knowing the value of M_z, H_0, and θ, the anisotropy constants K_1 and K_2 and g value have been calculated.

The classical equations of motion as first set up by Kittel have the form,

$$\left.\begin{aligned} dM_{x,y}/dt&=\gamma(\mathbf{M}\times\mathbf{H}_{\text{eff}})_{x,y}-(M_{x,y}/T_2),\\ dM_z/dt&=\gamma(\mathbf{M}\times\mathbf{H}_{\text{eff}})_z-[(M_z-M_0)/T_1].\end{aligned}\right\} \quad (6)$$

The relaxation terms are those used by Bloembergen and were based upon the form used by Bloch in describing nuclear magnetic resonance. An alternative form for these relaxation terms is that used by Yager *et al.* and first put forward by Landau and Lifshitz.[14] In the equation of motion this form appears as

$$d\mathbf{M}/dt=\gamma(\mathbf{M}\times\mathbf{H}_{\text{eff}})-(\gamma\alpha/M)[\mathbf{M}\times(\mathbf{M}\times\mathbf{H})]. \quad (7)$$

Since the physical mechanisms which lead to a broadening of the resonance line are not well understood, both of these damping terms have been introduced on purely empirical grounds.

The steady state solution of Eq. (6) yields

$$\mu''=\frac{4\pi\gamma^2M_0[H_0+(N_y{}^{a1}+N_y{}^{a2})M_0](2\omega/T_2)}{(-\omega^2+\omega_0{}^2)^2+(4\omega^2/T_2{}^2)}, \quad (8)$$

where we assume that $M_z=M_0$ and the sample is spherical so that $N_x=N_y=N_z$. Here $\omega_0{}^2=\gamma^2H^2{}_{\text{eff res}}$.

The solution of Eq. (7) is

$$\mu''=\frac{4\pi\dfrac{\alpha}{1+\alpha^2}\dfrac{\omega}{\gamma}\dfrac{1}{l_yH_z}\left[\dfrac{\omega^2}{\gamma^2}\dfrac{1}{l_xl_yH_z{}^2(1+\alpha^2)}+\dfrac{l_x}{l_y}\right]}{\left[1-\dfrac{\omega^2}{\gamma^2}\dfrac{1}{l_xl_yH_z{}^2(1+\alpha^2)}\right]^2+\dfrac{\alpha^2}{1+\alpha^2}\dfrac{(l_x+l_y)^2}{l_xl_y}\dfrac{\omega^2}{\gamma^2}\dfrac{1}{l_xl_yH_z{}^2(1+\alpha^2)}}\dfrac{M_0}{l_xH_z}, \quad (9)$$

where we have used Yager's notation that $l_xH_z=H_0+(N_x{}^{a1}+N_x{}^{a2})M_0$ and $l_yH_z=H_0+(N_y{}^{a1}+N_y{}^{a2})M_0$.

From either Eq. (8) or (9) we can calculate T_2 or its equivalent in terms of α by equating the peak value of μ'' as determined experimentally to the theoretical expression at resonance.

IV. RESULTS

The absorption resonance curves at several temperatures are shown in Fig. 3. The solid curves represent the theoretical curves where the damping term has been adjusted so that the value of μ'' at resonance agrees with the experimental value. For the room temperature data two sets of theoretical curves are drawn, one indicated by the solid curve and the other by solid triangles. The solid curve was drawn for the theoretical expression using a damping term of the form used by Bloembergen,[7] while the solid triangles are derived from the theoretical expression using the form of damping term used by Yager *et al.*[8] It is readily seen that there is is little difference between these two curves.

The room temperature data agree very well with those of Yager *et al.*[8] and give an absorption curve width of about 70 oersteds independent of the crystallographic orientation of the sample. At −195°C the width of the absorption curve is about 110 oersteds, and this decreases to about 50 oersteds at 588°C.

Figure 4 shows a plot of $1/T_2$ *vs* temperature. T_2 is the over-all relaxation time as determined from the width of the absorption curve. The decrease of $1/T_2$ with temperature was unexpected and is a different behavior from that observed in ferromagnetic metals. The fact that $1/T_2$ decreases with increase in temperature would suggest that spin lattice relaxation effects play only a small role in contributing to the over-all line width.

Figure 5 shows the variation of H_0 required for resonance measured as a function of the angle between the direction of H_0 and a [100] direction in the sample. In order to explain this angular variation it was necessary to include two anisotropy terms in the expression for the magnetic anisotropy energy. From the angular variation shown in Fig. 5, therefore, the anisotropy constants K_1 and K_2 were measured. Their variation with temperature is given in Fig. 6.

Referring again to Fig. 5, we have plotted a curve for 25°C showing the best fit to the observed angular variation of the resonant value of H_0 that can be made using only the first term in the expansion for the anistropy energy. We see that this curve does not fit the experimental data very well and that it is necessary to include the second-order term to get a good agreement. This result is different from that observed by

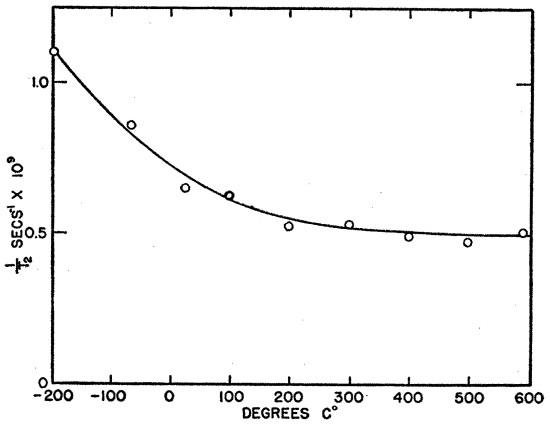

FIG. 4. $1/T_2$ *vs* temperature from $NiOFe_2O_3$ resonance curves.

[14] L. Landau and E. Lifshitz, Physik. Z. U.S.S.R. 8, 153 (1935).

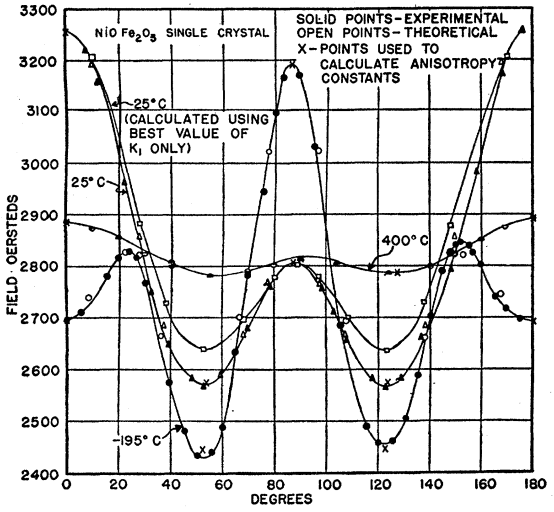

FIG. 5. H_{res} *vs* θ. θ equals angle in (110) plane between static field and cube edge.

Yager *et al.* and indicates that there may be considerable variation in the anisotropy energy from crystal to crystal depending on the impurity content and method of preparation.

Table I shows the variation in the g value as a function of temperature. This g value is calculated from the value of H_0 required for resonance and remains essentially constant over the whole temperature range. It had been expected that there would be some correlation between the value of g and that of the magnetic anisotropy energy. This correlation was expected since it is believed[15] that the spin system "feels" the crystal lattice through the agency of the spin-orbit and orbit-lattice coupling parameters. Thus any variation in the strength of the orbit-lattice coupling would be manifested by a change in both the g value and the anisotropy energy. Such a correlation is not evident here.

In calculating both the g values and the anisotropy constants it is necessary to know the saturation magnetization, M_0, of the nickel ferrite as a function of temperature. Pauthenet[16] has published data on this quantity. In experiments with other ferrities, however, it has been observed that there was considerable variation in both M_0 and the Curie temperature among ferrite samples of supposedly the same chemical composition. It was of interest, therefore, to ascertain the value of M_0 for the particular lot of $NiOF_2O_3$ crystals used here.

To do this some of the crystals used were ground to a fine powder and then formed into thin disk-shaped specimens by subjecting the powder to a pressure of several hundred tons per square inch in a hydraulic press. When the resonance phenomenon is observed for such samples it is found that the line width is considerably increased by the so-called "powder broadening." It is not expected that the resonant value of H_0 will be displaced due to this "powder broadening;" however, the resonant value of H_0 will be considerably affected by the demagnetizing field.

The demagnetizing field can be calculated using the formulas compiled by Osborne[17] considering the disks as limiting cases of flattened oblate spheroids. A value for M_0 can be determined by comparing the value of the field required for resonance in a spherical sample, where M_0 enters only through the anisotropy field, with the field required for resonance in a disk-shaped sample, which is strongly affected by M_0 through the agency of the demagnetizing fields. Figure 7 shows the temperature variation of M_0 calculated in this fashion compared with the data prepared by Pauthenet.

Table I also lists the g value computed for the disk-shaped samples using the calculated value of M_0. These values of g are quite sensitive to any error in determining M_0 and thus agree with the values of g computed for the spherical samples within the accuracy of the experiment. In addition, we have listed in Table I the value of H_0 required for resonance and the computed value of H_{eff}.

V. CONCLUSIONS

Comparison of the experimental data with the curves predicted by Kittel's theory shows that a resonance type curve fits the observations very well. The physical reasons for this are not clear. Measurements made by Damon[18] on spin-lattice relaxation times indicate that the spin lattice interaction contributes little to the line width. Since the other mechanisms which are responsible for the line width are not evident, it seems fruitless to discuss the more difficult problem of line shape.

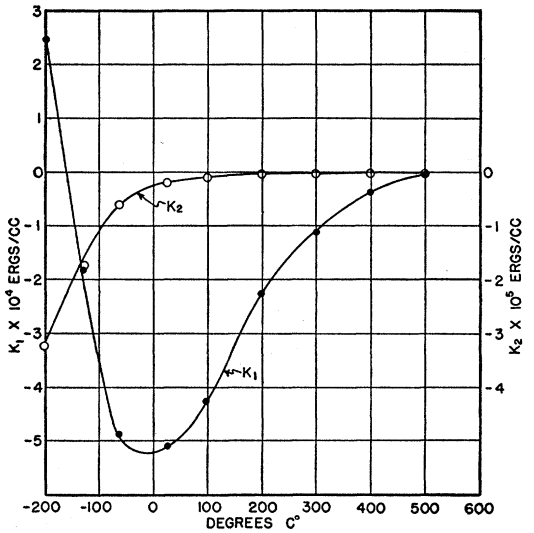

FIG. 6. K_1 and K_2 *vs* temperature ($NiOFe_2O_3$).

[15] J. H. Van Vleck, Phys. Rev. **52**, 1178 (1937).
[16] R. Pauthenet, Compt. rend. **230**, 1842 (1950).
[17] J. A. Osborne, Phys. Rev. **67**, 351 (1945).
[18] R. W. Damon, Ph.D. thesis, Harvard University (1951).

The increase of T_2 with temperature shown in Fig. 4 is unexpected. This increase rules out the possibility that spin lattice relaxation and dipolar forces contribute materially to the line width since their temperature variation would be the inverse of that observed. The fact that the line width increases along with the increase in ordering of the electron spins, as 0°K is approached, indicates that the cause for the line broadening might be sought in action of the pseudo-dipolar forces mentioned by Van Vleck.[3] He points out that, if crystalline imperfections exist, these forces may couple together microcrystals of slightly different resonance frequencies, thus broadening the line. Such forces could increase with the increase in anisotropy energy and thus become more pronounced at low temperatures.

In this connection it would be of interest to make measurements at lower temperatures to determine whether or not ordering of the magnetic lattice eventually overcomes the tendency for the line to broaden. It may be, as Van Vleck suggested, that the effect of impurities in the crystal lattice would obscure such tendency and no narrowing would be observed.

Experiments at lower temperature would likewise be of interest in connection with the anisotropy energy. The measurements made here show that the anisotropy

TABLE I. g values of $NiOFe_2O_3$.

Single crystal sphere				Polycrystalline material	
Temp	H_{res}	H_{eff}	g	Temp	g
−195°C	2486	2856	2.26	−195°C	2.28
−65°C	2567	2878	2.24		
25°C	2597	2866	2.25	25°C	2.24
100°C	2677	2878	2.23	115°C	2.19
200°C	2693	2834	2.26	233°C	2.20
300°C	2735	2844	2.25	360°C	2.16
400°C	2792	2828	2.26	488°C	2.20
500°C	2795	2813	2.27	542°C	2.30
588°C	2813	2812	2.27		

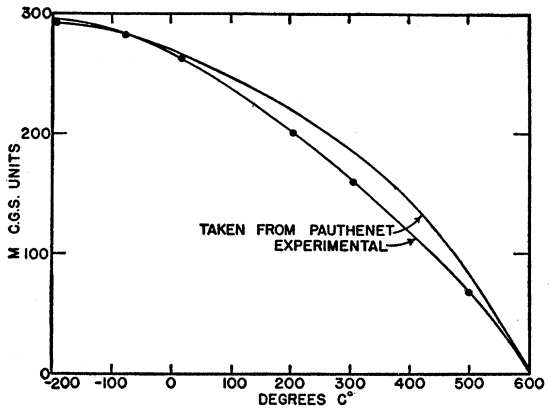

FIG. 7. M *vs* temperature for $NiOFe_2O_3$ polycrystalline material.

constants increase in magnitude very rapidly with temperature in the vicinity of −195°C, and it is not expected that such a temperature variation would continue. At higher temperatures, as has been observed in the ferromagnetic metals, the anisotropy energy falls to zero before the Curie temperature is reached.

The g value as seen from Table I remains essentially constant over the whole temperature range studied. This is a different behavior from that reported by Bickford[6] for magnetite. In the case of magnetite the change in g value could be correlated with the change in anistropy energy, the lowest g value occurring near the temperature where magnetite undergoes a transition and becomes magnetically isotropic. No such correlation is possible here, and reasons for this different behavior are not known.

In conclusion the writer would like to acknowledge his debt to Professor N. Bloembergen who has given generously of his time and advice during this investigation. He would also like to acknowledge his gratitude to the Bell Telephone Laboratories who supplied the single crystals of $NiOFe_2O_3$ studied.